Research Square

Preprints are preliminary reports that have not undergone peer review.
They should not be considered conclusive, used to inform clinical practice,
or referenced by the media as validated information.

Enhanced Near-Infrared Sensitivity and Extended Detection Wavelength in Silicon Phototransistors Using a Backside Aluminum Reflector

Yu-Jin Cho
Chungbuk National University
Hyeong-Soo Kim
Chungbuk National University
Moon Hee Kang
moonhee@chungbuk.ac.kr

Chungbuk National University

Research Article

Keywords: Silicon phototransistors, Near-infrared detection, Backside metal reflector, Optical confinement

Posted Date: October 1st, 2026

DOI: https://doi.org/10.21203/rs.3.rs-11109142/v1

License: This work is licensed under a Creative Commons Attribution 4.0 International License.
Read Full License

Additional Declarations: No competing interests reported.

Abstract

Silicon-based phototransistors are often used for near-infrared (NIR) sensing because of their low cost and complementary metal-oxide semiconductor (CMOS) compatibility. However, their NIR detection capabilities are limited by the weak optical absorption of Si at long wavelengths. In this study, a simple backside Al reflector was introduced to enhance the NIR photoresponse of metal-oxide-semiconductor field-effect transistor-type Si phototransistors. The incorporation of the backside Al reflector extended the detectable wavelength range from 1200 to 1300 nm. The responsivity increased by more than 12 times in the 900–1100 nm range, and by approximately 26 times at 1300 nm. Additionally, the dark current was reduced from 2.5×10^{-10} A to 5.4×10^{-12} A, corresponding to a 46-fold reduction, while maintaining comparable on-state current characteristics. Finite-difference time-domain simulations revealed that the backside Al reflector enhances light utilization within the Si substrate by reflecting the transmitted photons back into the active region, leading to an increased optical power density at longer wavelengths. These results demonstrate that implementing a simple, CMOS-compatible backside reflector is an effective strategy for substantially enhancing the NIR photoresponse of Si phototransistors and extending their practical detection limit into the weak-absorption regime up to 1300 nm.

1. Introduction

Silicon-based phototransistors have been extensively used in optoelectronic applications because of their low fabrication cost and compatibility with mature complementary metal-oxide semiconductor (CMOS) processes. Nevertheless, their photoresponse gradually deteriorates in the near-infrared (NIR) region owing to the decreasing absorption coefficient of Si at long wavelengths [1, 2]. Thus, a significant fraction of incident NIR photons are not absorbed within the active region, limiting photocurrent generation and responsivity.

Several approaches have been explored to improve the NIR performance beyond this intrinsic limitation. Defect-assisted absorption, bandgap narrowing induced by heavy doping [1], and impurity-state engineering have been extensively investigated. This has led to one approach that focuses on modifying the electronic structure of the phototransistor to enable sub-bandgap photon absorption. For example, Wang et al. demonstrated infrared (IR) absorption beyond the intrinsic Si bandgap using Mg- or Te-doped Si [3, 4]. Other studies have reported that deep-level impurities introduced through impurity doping followed by pulsed laser melting can significantly enhance the broadband IR absorption in Si [5]. Schottky phototransistors based on internal photoemission mechanisms have been extensively studied. In these devices, sub-bandgap photons can be detected through carrier emission across the Schottky barrier, thereby enabling a photoresponse beyond the intrinsic absorption limit of Si [6–10]. Although these approaches can extend the detectable wavelength range, they often suffer from an increased dark current, reduced signal-to-noise ratio, or additional fabrication complexity.

As an alternative to electronic structure modification, optical engineering strategies have been explored to enhance the NIR photoresponse while preserving the intrinsic electrical characteristics of Si devices. Resonant cavity structures [11, 12] and plasmonic configurations [9, 13] have been proposed to increase the effective optical path length and improve light absorption within the Si absorber. Although these approaches can effectively enhance NIR sensitivity, they often require sophisticated nanostructures or complex fabrication processes. Therefore, a simple optical approach that improves light confinement without substantially increasing the fabrication complexity is highly desirable.

Among the different optical engineering approaches, backside metal reflectors [14] provide a simple and scalable solution for enhancing NIR light absorption. By reflecting the photons transmitted back onto the Si substrate, the effective optical path length can be increased, thereby improving the probability of photon absorption and photocarrier generation. In this study, a backside Al reflector was used to enhance the NIR performance of metal-oxide-semiconductor field-effect transistor (MOSFET)-type Si phototransistors. The proposed structure increases the optical confinement through a multi-pass absorption mechanism, resulting in an enhanced photocurrent and responsivity in the NIR wavelength range. Additionally, the increased optical absorption contributes to maintaining a measurable photoresponse at longer wavelengths compared to devices without a reflector. The optical and electrical characteristics of the fabricated devices were systematically investigated to evaluate the effectiveness of the proposed approach and elucidate the underlying enhancement mechanisms.

2. Experimental

A. Fabrication of the Phototransistor

Figure 1 shows the process-flow for the fabrication of the phototransistor. The MOSFET-type NIR phototransistors were fabricated on 4-inch, (100)-oriented boron-doped p-type Si wafers with a resistivity of ~ 1 Ω·cm. The native oxide was removed using a buffered oxide etchant solution, followed by the growth of a 10 nm-thick SiO_2 gate dielectric through thermal dry oxidation to provide a high-quality Si–SiO_2 interface. A 100 nm-thick in-situ phosphorus-doped polycrystalline silicon (poly-Si) layer with a doping concentration of 2×10^{20} cm^{-3} was then deposited by low-pressure chemical vapor deposition. The poly-Si gate electrode was then patterned using reactive-ion etching at Ar/CF_4 gas flow rates of 15/135 sccm, respectively, radio frequency power of 300 W, and etching time of 105 s. The fabricated devices used an enclosed-gate structure with a channel 40 μm long and 260 μm wide. After gate formation by photolithography, arsenic ions were implanted at 40 keV with a dose of 5×10^{15} cm^{-2} to form heavily doped n^+ source and drain regions. Rapid thermal annealing was then performed at 1000°C for 15 s to activate the implanted dopants and repair the implantation-induced lattice damage. Prior to the Al deposition, a pre-sputtering process was performed for 300 s under an Ar flow rate of 20 sccm to remove contaminants and stabilize the plasma. To enhance optical absorption in the NIR wavelength range, a 100 nm-thick Al (optical reflecting) layer was then deposited on the backside of the wafer by sputtering for 720 s under identical Ar-flow conditions

The electrical and photoresponse characteristics of the fabricated devices were measured using a semiconductor parameter analyzer (Keithley 4200A-SCS) under dark and illuminated conditions. Monochromatic NIR light in the wavelength range of 900–1300 nm was generated using a tungsten–halogen lamp coupled to a monochromator. The light was guided onto the device through a $600\ \mu\mathrm{m}$ core-diameter multimode optical fiber, with the total incident optical power calibrated to approximately $10\backslash:\mathrm{mW}$ at each wavelength, yielding an optical power density of ~ 3.54 W/cm^2.

B. Device Structure of the Phototransistor

Figure 2 shows the fabricated MOSFET-type NIR phototransistor. Figure 2(a) shows an optical microscopy image of the fabricated device. An enclosed-gate structure was adopted to suppress the edge leakage current and improve device stability during photodetection. The fabricated device had a width of 300 μm and a length of 500 μm. Figure 2(b) presents a top-view scanning electron microscopy (SEM) image of the device structure, which clearly identifies the gate, source, and drain regions. Figure 2(c) presents a cross-sectional SEM image of the gate stack and Si substrate. The thickness of the phosphorus-doped poly-Si gate was approximately 105.9 nm.

As described above, the device was fabricated using a CMOS-compatible process, enabling potential integration with conventional Si-based electronic platforms. In addition to its process compatibility, the phosphorus-doped poly-Si gate provides optical advantages for NIR photodetection. Unlike metal gate electrodes that are highly reflective and optically opaque in the NIR wavelength range, poly-Si gates exhibit partial optical transparency, allowing incident photons to penetrate the gate electrode and reach the underlying Si substrate. As a result, a larger fraction of the incident NIR light can be coupled to the Si substrate, increasing the probability of photon absorption and photocarrier generation.

3. Results and discussion

A. Electrical and Optical Characteristics of the Phototransistor

Figure 3 shows the transfer characteristics of the fabricated MOSFET-type NIR phototransistors measured at V_{DS} = 0.1 V under dark and monochromatic NIR illumination (900–1300 nm), with an incident optical power of approximately 10 mW. Figure 3(a) and 3(b) correspond to devices without and with a backside Al reflector, respectively.

For the phototransistor without the backside Al reflector, distinct photoresponses are observed at illumination wavelengths of 900–1200 nm. As the illumination wavelength increases, the photocurrent gradually decreases because of the reduced absorption coefficient of Si near the absorption edge. At 1300 nm, the transfer characteristics become almost indistinguishable from the dark-current curve, indicating that the incident photons are not effectively detected.

By contrast, the phototransistor incorporating the backside Al reflector exhibits significantly enhanced photoresponse characteristics over the entire measured wavelength range. The separation between the

illuminated and dark transfer curves becomes more pronounced, indicating an improved photocarrier generation. Clear photoresponses are maintained even at 1300 nm, whereas the device without a reflector exhibits a negligible response. These results demonstrate that the detectable wavelength range is extended from 1200 to 1300 nm by incorporating the backside Al reflector.

The enhanced photoresponse is attributed to the optical reflection provided by the backside Al layer. NIR photons that are not absorbed during their initial propagation through the Si substrate are reflected into the active region, thereby effectively increasing the optical path length. This light-trapping effect enhances the photon absorption and photocarrier generation, particularly at longer wavelengths where the absorption coefficient of Si is inherently low. Consequently, the backside Al reflector significantly improves the NIR sensitivity of the phototransistor and extends the measurable NIR detection range up to 1300 nm by enhancing multi-pass absorption.

Figure 4 shows the wavelength-dependent responsivity (R) and specific detectivity (D^*) of the MOSFET-type NIR phototransistors with and without a backside Al reflector. The spectral responsivity was evaluated as $R = \left(I_{light} - I_{dark}\right) / P_{in}$, where P_{in} is the incident optical power. Assuming that the shot noise from the dark current is the dominant noise source, the specific detectivity was calculated using $D^* = \frac{R\sqrt{Area}}{\sqrt{2qI_{dark}}}$. For the device without the reflector, the responsivity generally decreases as the wavelength increases, reflecting the reduced absorption coefficient of Si near its band edge. The responsivity decreases from 5.7×10^{-7} A/W at 900 nm to 1.6×10^{-9} A/W at 1300 nm. The corresponding specific detectivity also decreases from 1.0×10^{5} Jones to 2.9×10^{2} Jones. The backside Al reflector substantially enhances the responsivity over the measured wavelength range. In the 900–1100 nm wavelength range, the responsivity is enhanced by more than 13 times compared with that of the device without the reflector. At 900, 1000, 1100 nm, the responsivity increases from 5.7×10^{-7}, 4.1×10^{-7}, and 9.5×10^{-8} A/W to 8.5×10^{-6}, 5.3×10^{-6}, and 1.2×10^{-6} A/W, respectively. This improvement is attributed to the increased optical path length and enhanced light absorption resulting from the reflection of transmitted photons at the backside Al layer. The enhancement becomes more pronounced with increasing wavelength, reaching its maximum at 1300 nm. At this wavelength, the responsivity increases from 1.6×10^{-9} A/W without the reflector to 4.3×10^{-8} A/W with the reflector, corresponding to an enhancement of approximately 27 times. Although the absolute responsivity at 1300 nm remains relatively low owing to the inherently weak band-tail absorption in thin Si layers, the simultaneous 46-fold suppression of dark current allows the device with the Al reflector to achieve a meaningful specific detectivity of 2.0×10^{5} Jones. This demonstrates that the measurable photoresponse can be reliably distinguished from the electrical noise floor even in the weak-absorption regime. The enhancement is even more pronounced in terms of specific detectivity due to the synergistic effect of responsivity improvement and dark-current reduction. The specific detectivity of the device with the backside Al reflector reaches 4.0×10^{7} Jones at 900 nm (compared to 4.0×10^{5} Jones without Al) and remains consistently superior across all measured wavelengths, confirming high-sensitivity and low-noise NIR photodetection capability.

In addition to the enhanced photoresponse, the incorporation of the backside Al reflector results in a noticeable reduction in the dark current, as observed in Fig. 5. To quantitatively assess this reduction, the dark current was extracted at V_G = − 0.75 V, where the minimum dark current was observed. The dark current decreases from 2.5×10^{-10} A to 5.4×10^{-12} A after the introduction of the backside Al layer, corresponding to a 46-fold reduction in dark current. By contrast, the on-state current remains comparable after the incorporation of the backside Al reflector, indicating that the backside Al layer effectively suppresses the leakage current without degrading the intrinsic channel-transport characteristics of the MOSFET phototransistor.

Figure 5 summarizes the statistical distribution of dark currents extracted from multiple devices. The phototransistors incorporating the backside Al reflector consistently exhibit lower dark current values than those without the reflector. The median dark current is reduced by one order of magnitude, confirming that the observed reduction is reproducible and not caused by device-to-device variation. These results demonstrate that the backside Al reflector not only enhances the NIR photoresponse, but also contributes to low-noise operation by significantly suppressing the dark current.

The significant reduction in the dark current is attributed to the presence of the backside Al layer. In addition to serving as an optical reflector, the Al layer may modify the electrical boundary condition at the backside of the Si substrate, which can influence the carrier transport and leakage pathways under off-state conditions. Consequently, the incorporation of the backside Al reflector contributes to the suppression of leakage current while maintaining normal device operation. Importantly, the on-state current remains comparable after the introduction of the backside Al reflector, indicating that the intrinsic channel transport characteristics of the MOSFET phototransistor are largely preserved. This suggests that the dark current is reduced without significantly affecting carrier transport in the surface channel. These results demonstrate that the backside Al reflector provides a dual benefit: enhanced NIR photoresponse through optical path length extension and substantially reduced dark current. Consequently, the proposed structure enables high-sensitivity and low-noise NIR photodetection.

B. Optical Field Distribution and Light-Trapping Effect of the Backside Al Reflector

To investigate the origin of the enhanced photoresponse, finite-difference time-domain (FDTD) simulations were performed using luminous FDTD solutions, as shown in Fig. 6. For the device without a backside Al reflector, a significant portion of the incident light propagates through the Si substrate and is lost by transmission. This results in relatively weak optical power within the Si region, particularly at longer wavelengths. Contrastingly, the device incorporating the backside Al reflector exhibits a noticeably higher optical power density within the Si substrate, owing to the reflection of the transmitted light at the backside interface. This enhancement becomes more pronounced as the wavelength increases. Particularly, the device with the backside Al reflector maintains a higher optical power distribution in the Si region at wavelengths above 1100 nm, where the absorption coefficient of Si is significantly reduced. These results indicate that the backside Al reflector effectively improves light

utilization within the Si substrate and are consistent with the experimentally observed enhancement in responsivity and extension of the detectable wavelength range.

4. Conclusion

In this study, a backside Al reflector was introduced to enhance the NIR photoresponse of Si-MOSFET-type phototransistors. The incorporation of the backside Al reflector extends the detectable wavelength range from 1200 to 1300 nm and increases the responsivity by more than 12 times in the 900–1100 nm range and by approximately 26 times at 1300 nm. Additionally, the dark current is reduced by approximately 46 times while maintaining comparable on-state current characteristics. FDTD simulations confirm that the enhanced performance originates from the improved light utilization within the Si substrate owing to reflection from the backside Al layer. These results demonstrate that the proposed backside reflector structure provides a simple and CMOS-compatible approach for extending the NIR detection capability of Si phototransistors into the weak-absorption regime up to 1300 nm.

Declarations

Author Contribution

Yu-Jin Cho conducted the experiments, analyzed the data, and wrote the initial draft of the manuscript. Hyeong-Soo Kim assisted with the experiments. Moon Hee Kang supervised and managed the project and reviewed and revised the manuscript. All authors reviewed and approved the final manuscript.

Acknowledgments

This work was supported by the National Research Foundation of Korea(NRF) grant funded by the Korea government(MSIT) (No. RS-2024-00355125)

This research was supported by the Regional Innovation System & Education(RISE) program through the Chungbuk Regional Innovation System & Education Center funded by the Ministry of Education(MOE) and the Chungcheongbuk-do, Republic of Korea (2026-RISE-11-014-03).

References

1. S.M. Sze, Physics of Semiconductor Devices, John Wiley & Sons, Inc., 1981.
2. M.A. Green, Solar cells: operating principles, technology, and system applications, Prentice-Hall, Inc., Englewood Cliffs, NJ, 1982.
3. M. Wang, M.S. Shaikh, U. Kentsch, R. Heller, S. Zhou, Sub-band gap infrared absorption in Si implanted with Mg, Semicond. Sci. Technol. 38 (2023). https://doi.org/10.1088/1361-6641/aca3ca.

4. M. Wang, Y. Berencén, E. García-Hemme, S. Prucnal, R. Hübner, Y. Yuan, C. Xu, L. Rebohle, R. Böttger, R. Heller, H. Schneider, W. Skorupa, M. Helm, S. Zhou, Extended Infrared Photoresponse in Te - Hyperdoped Si at Room Temperature, Phys. Rev. Appl. 10 (2018). https://doi.org/10.1103/PhysRevApplied.10.024054.
5. J. Fu, D. Yang, X. Yu, Hyperdoped Crystalline Silicon for Infrared Photodetectors by Pulsed Laser Melting: A Review, Physica Status Solidi (A) Applications and Materials Science 219 (2022). https://doi.org/10.1002/pssa.202100772.
6. Y. Jin, J. Seok, K. Yu, Highly Efficient Silicon-Based Thin-Film Schottky Barrier Photodetectors, ACS Photonics 10 (2023) 1302–1309. https://doi.org/10.1021/acsphotonics.2c01923.
7. D. Dudi, S. Ram Prakash, K. Bhardwaj, B. Aïssa, A. Mitra, Ni/n-Si Schottky junction: Self-biased infrared photodetection via hot carrier photoemission, Optik (Stuttg). 318 (2024) 172093. https://doi.org/https://doi.org/10.1016/j.ijleo.2024.172093.
8. P. Ji, S. Yang, Y. Wang, K. Li, Y. Wang, H. Suo, Y.T. Woldu, X. Wang, F. Wang, L. Zhang, Z. Jiang, High-performance photodetector based on an interface engineering-assisted graphene/silicon Schottky junction, Microsyst. Nanoeng. 8 (2022). https://doi.org/10.1038/s41378-021-00332-4.
9. W. Zhou, X. Liu, T. Shi, Z. Li, F. Yan, H. Zhou, Y. Liao, X. Ji, Multilayer Plasmonic Structure-Enhanced Near-Infrared CoSi 2 /Si Schottky Photodetector via Standard CMOS Process, ACS Photonics (2025). https://doi.org/10.1021/acsphotonics.5c00968.
10. K.H. Sharma, Y.H. Dong, P.H. Chiang, Z.C. Su, C.F. Lin, Silicon (100) surface passivation-driven tuning of Ag film crystallinity and its impact on the performance of Ag/n-Si mid-infrared Schottky photodetector, APL Mater. 12 (2024). https://doi.org/10.1063/5.0214341.
11. M. Casalino, Design of Resonant Cavity-Enhanced Schottky Graphene/Silicon Photodetectors at 1550 nm, Journal of Lightwave Technology 36 (2018) 1766–1774. https://doi.org/10.1109/JLT.2018.2791720.
12. M. Casalino, G. Coppola, M. Gioffre, M. Iodice, L. Moretti, I. Rendina, L. Sirleto, Cavity enhanced internal photoemission effect in silicon photodiode for sub-bandgap detection, Journal of Lightwave Technology 28 (2010) 3266–3272. https://doi.org/10.1109/JLT.2010.2081346.
13. F. Alihosseini, A.R. Zali, T. Pakizeh, H. Zandi, Plasmonic internal-photoemission-based Si photodetector design suitable for optical communication, Appl. Opt. 61 (2022) 6939–6946. https://doi.org/10.1364/AO.462171.
14. J. Cui, Z. Zhou, High-performance Ge-on-Si photodetector with optimized DBR location, Opt. Lett. 42 (2017) 5141–5144. https://doi.org/10.1364/OL.42.005141.

Figures

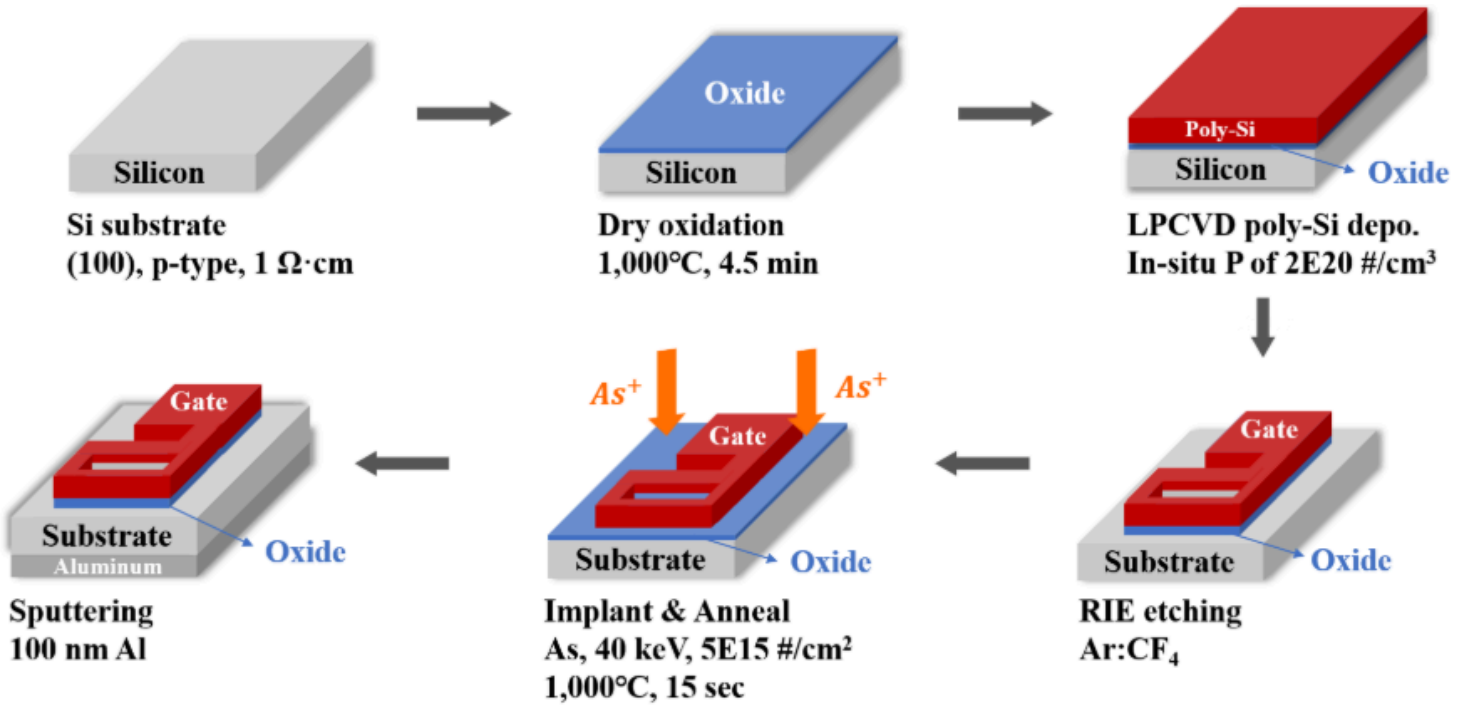


Figure 1

Process flow for the fabrication of the MOSFET-type NIR phototransistor with a backside Al reflector.

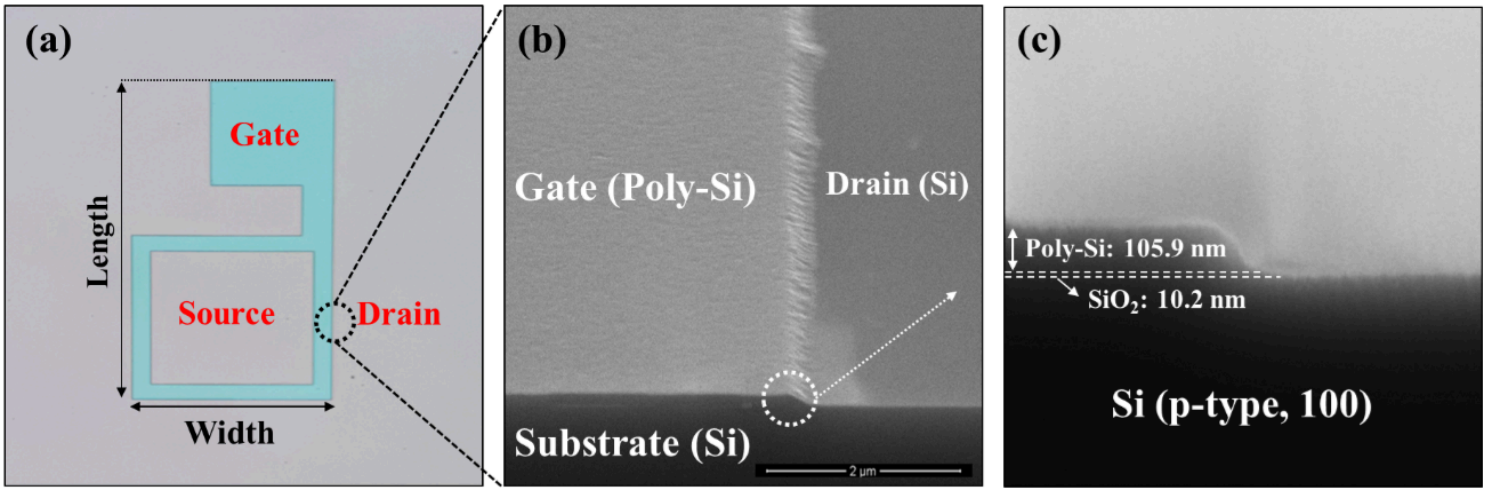


Figure 2

(a) Optical microscope image of the fabricated MOSFET-type NIR Phototransistor; (b) Top-view SEM image of the device structure; (c) Cross-sectional SEM image of the gate stack and Si substrate.

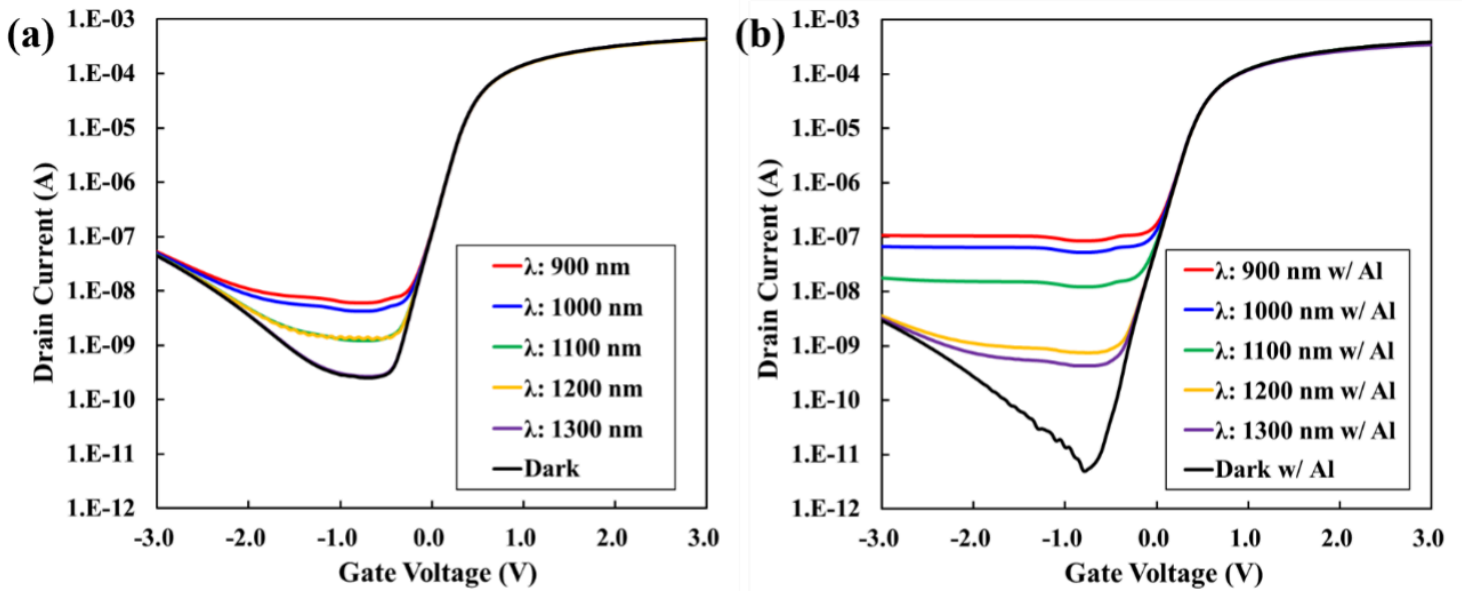


Figure 3

Transfer characteristics of the fabricated MOSFET-type NIR phototransistors measured at V_{DS} = 0.1 V: (a) Phototransistor without a backside Al reflector; (b) Phototransistor with a backside Al reflector.

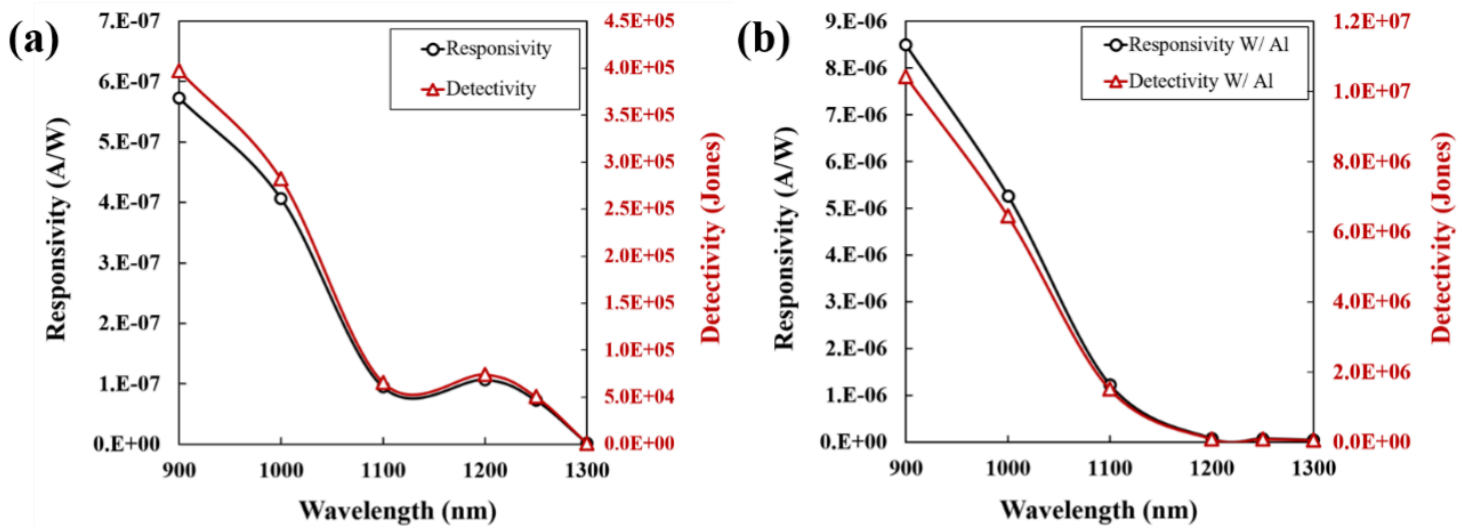


Figure 4

Wavelength-dependent responsivity and detectivity of MOSFET-type NIR phototransistors (a) without and (b) with a backside Al reflector.

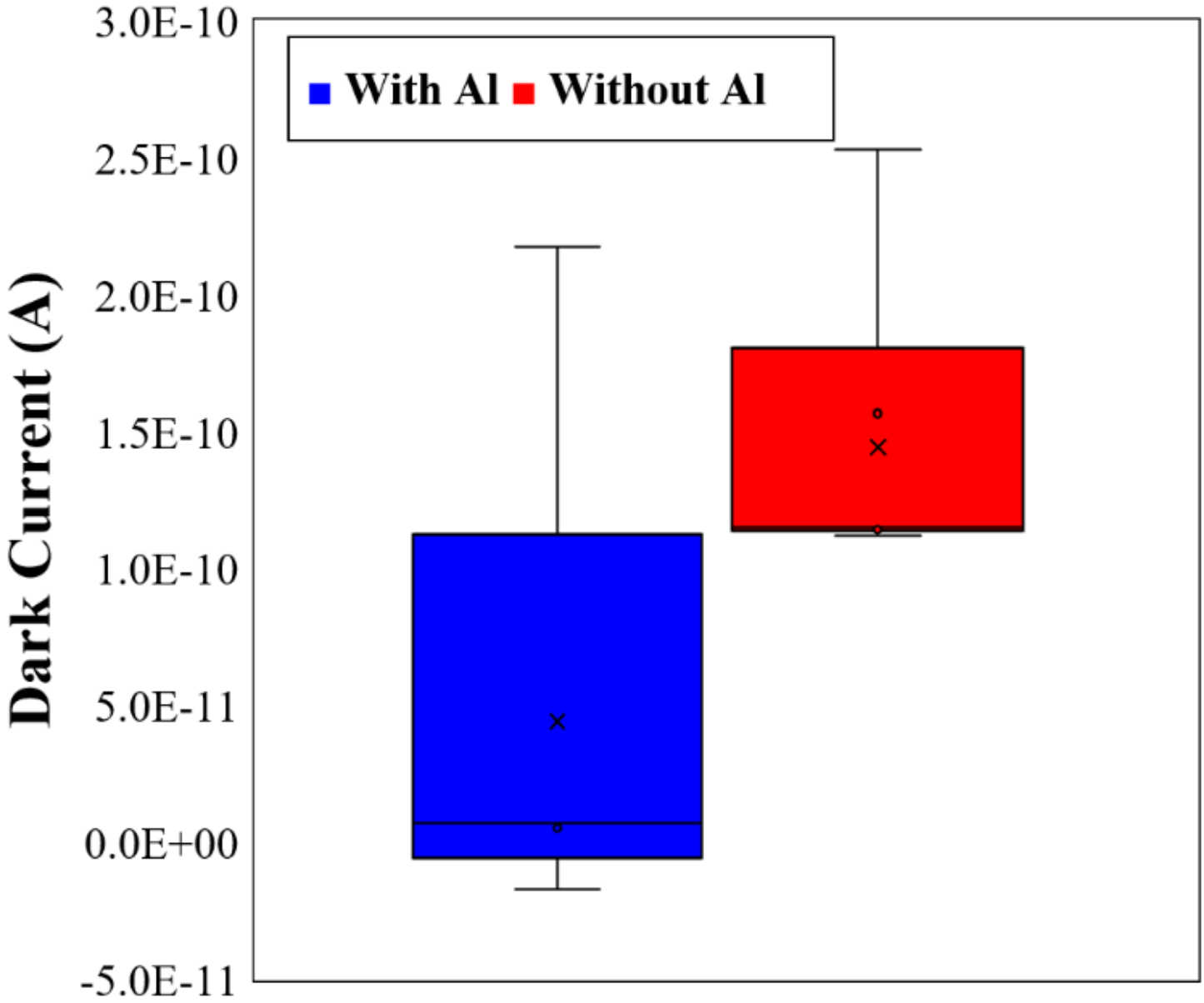


Figure 5

Statistical distribution of the dark current extracted from multiple phototransistors at V_G = -0.75 V and V_{DS} = 0.1 V.

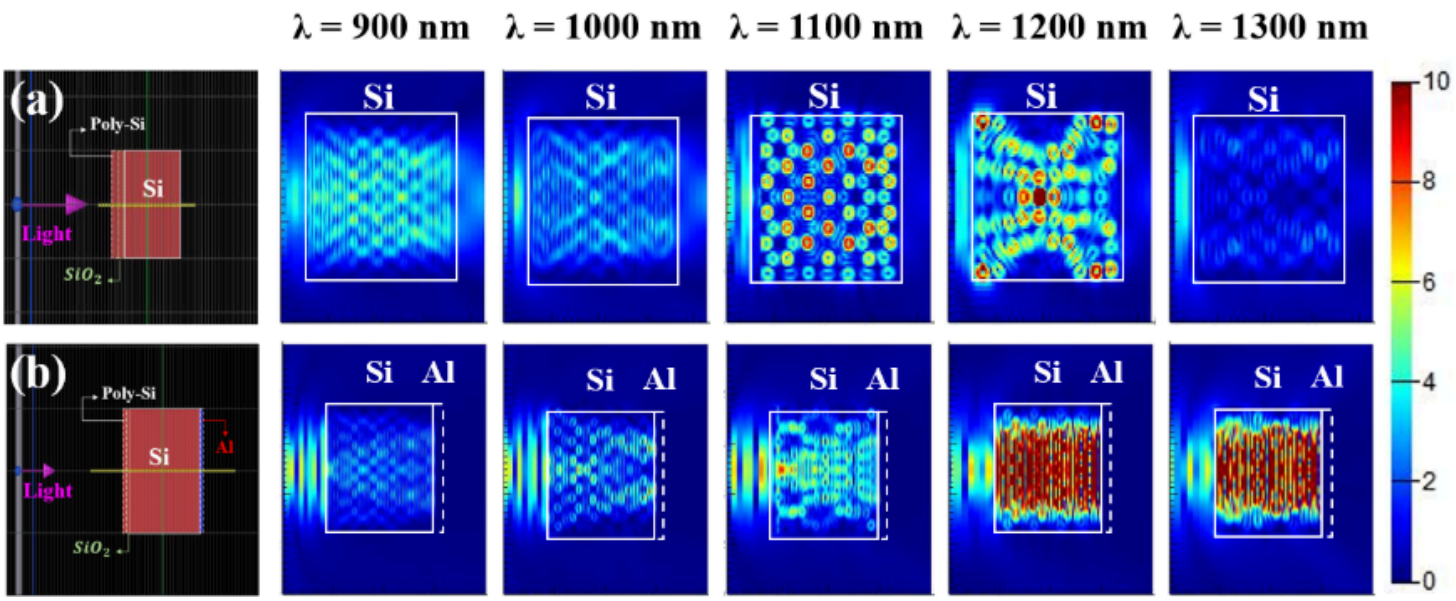


Figure 6

FDTD-simulated optical power distributions of the MOSFET-type NIR phototransistors: (a) Without a backside Al reflector; (b) With a backside Al reflector.